INTRODUCTION

This paper shows how to compute vibrations of rectangular elastic plates with random inhomogeneous parameters. The elastic plates here include a single plate with various random stiffness distributions and a double-leaf plate (DLP) with irregular junctions between the plates and the reinforcement beams. Figures 1 and 2 show simple depictions of the structures studied in this paper. Numerical simulations will be used to study the variations of the fundamental frequencies of the single-plate when the plate has different kinds of random rigidity. The DLP will be studied using the same randomness in addition to the randomness in the junctions. The displacement of the two plates will be computed, and then the transmission loss between the two plates will be studied.

Some elastic plates with random material properties such as rigidity or density may be studied using the theory of random matrices. Though, the random matrix theory can be rather technical and it usually deals with distributions of whole eigenvalues of very large matrices. In this paper the stiffness matrices are small because of the finite size and the simple rectangular shape of the plates. Figure 1 shows an example of discrete random rigidity distributed over the grid on the plate. The rigidity D_{pq} is a random variable with some probability density function (PDF). It is simple to run numerical experiments to confirm that the eigenvalues or the fundamental frequencies are normally distributed when D_{pq} has either a uniformly and a normally distributed PDF. However the distribution of fundamental frequencies behaves differently when the rigidity varies smoothly over the plate with smooth power spectral density.

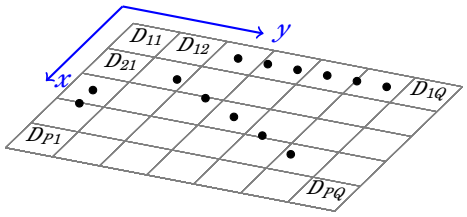

FIGURE 1: Depiction of the randomly distributed rigidity.

The number of components in a DLP (see Fig. 2), which have to be connected in some ways, makes it difficult to construct mathematical models of DLPs. Although DLPs are theoretically difficult to deal with, they are attractive in real-life. DLPs have high strength-to-weight ratio, and are used in many lightweight constructions. A difficulty of modelling a DLP is that components interact in complex and unpredictable ways. There are various methods of joining the two component, such as nails and glue, which are difficult to represent mathematically. An often used modelling method is the finite element method (FEM), which requires detailed descriptions of the junction between a plate and a beam, e.g., nail's reacts to forces and affects the surrounding material.

In this paper the displacement of the plates is found using the Fourier expansion of the solution, which is possible here because of the rectangular shape of the DLP. The Fourier expansion method requires less computation than FEM. Furthermore the conditions at the junctions, which must be functions of spatial variable(s), can be included in the variational formulation as the Fourier expansion. The reduction of computation time leads to faster Monte-Carlo simulations. It may be computationally impossible to use the FEM to perform 1000s of Monte-Carlo simulations over wide frequency range without a super computer. Whereas all results shown here are produced using MatLab on an average desktop PC.

Deterministic models of plates-and-beams can predict the vibrations of DLPs of various types as shown in, for example (Brunskog, 2005; Chung and Emms, 2008; Mace, 1980; Wang *et al.*, 2005). These papers have also shown shortcomings of deterministic models at higher

frequencies. As an alternative to the FEM, the statistical energy analysis (SEA) (see (Lyon, 1975)) has been developed and used often to study the wave propagation through complex structures. SEA can predict the high frequency surface vibration. Some argument against using the SEA in the low-to-mid-frequency range is given in (Fahy, 1994). An example of SEA's unsuitability in predicting energy propagation in a DLP is given in (Brunskog and Chung, 2011).

METHODS OF SOLUTION

Single plate and DLP

The method of solutions comes directly from Hamilton's principle for elastic plates (see (Shames and Dym, 1991)), which states that when there is an external force that causes the plate to vibrate the total energy (Lagrangian) of the plate satisfies the following equation for the first variation of the time integral of the Lagrangian.

$$\delta^{(1)} \int_{t_1}^{t_2} (\mathscr{T} - \mathscr{V} - \mathscr{U})\, dt = 0 \tag{1}$$

where $\mathscr{T}$, $\mathscr{V}$ are the kinetic and strain energies and $\mathscr{U}$ is the work done to the plate by the external force. For simplicity the simple harmonic oscillation of a thin plate is considered here. Thus the solution or the vertical displacement of the mid-plane of the plate is given by the real function $\mathbf{Re}\left[w(x,y)e^{\mathrm{i}\omega t}\right]$, where $\omega = 2\pi\alpha$ is the radial frequency for the frequency α in Hz. Then mathematical formulations can be simplified for the function $w(x,y)$ because of the linearity of the thin-plate theory. The integral over time in Eq. (1) is unnecessary. The displacement $w(x,y)$ will be defined for $(x,y) \in [0,A] \times [0,B]$, which is the size of the rectangular plate here. Hence the terms in the integral are completely determined by the vertical displacement of the plate.

The strain energy and kinetic energy of a plate with non-moving boundaries are

$$\mathscr{V} = \frac{1}{2}\int_0^A \int_0^B D(x,y)\left|\nabla^2 w(x,y)\right|^2 dxdy,\ \mathscr{T} = \frac{\rho h\omega^2}{2}\int_0^A \int_0^B |w(x,y)|^2 dxdy \tag{2}$$

where $D(x,y) = E(x,y)h^3/\left(12\left(1-\nu^2\right)\right)$ is the flexural rigidity, and h, E, and ν are the plate thickness, Young's modulus and Poisson's ratio, respectively. Note that the effects of rotation are neglected in $\mathscr{T}$. The work done to the plate is given by the following integral when the external force is distributed over the plate by the function $p(x,y)$.

$$\mathscr{U} = \int_0^A \int_0^B p(x,y)w(x,y)dxdy \tag{3}$$

An additional plate joined by parallel reinforcement beams can be included in the modelling using the same variational formulation. The additional components' strain and kinetic energies can be included in the integral form in Eq. (2). The displacements of the top and the bottom plates are denoted by $w_1(x,y)$ and $w_3(x,y)$, respectively. The displacements of the beams are denoted by $w_2(x,j)$, where $j = 1,2,...,S$ indicates jth beam located at $y = y_j$. Note that the beams here are assumed to be always in contact with the plates. It is possible to add more degrees of freedom to the beams as shown in (Chung, 2012), though we consider only the lateral slippage between the plates and the beams. The Kinetic and the strain energies of the plates have the same formulas as Eq. (2) for w_3.

The beams will be modelled using the Euler beam theory. Thus the strain and kinetic energy contributions from the beams are

$$\mathscr{V}_2 = \frac{1}{2}\sum_{j=1}^{S}\int_0^A D_2\left|w_2''(x,j)\right|^2 dx,\ \mathscr{T}_2 = \frac{\rho_2 h_2\omega^2}{2}\sum_{j=1}^{S}\int_0^A |w_2(x,j)|^2 dx \tag{4}$$

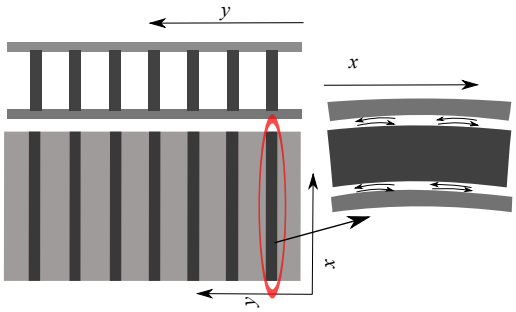

FIGURE 2: Depiction of double-plate model.

where D_2 is the rigidity of the beam and ρ_2 and h_2 are the mass density per unit length and the thickness of the beam, respectively. Note that the primes on w_2 indicate the second derivative with respect to x. Here D_2 is assumed to constant and calculated using the formula $D_2 = E_2 h_2^3 l/12$, where E_2, h_2 and l are the Young's modulus, vertical depth and horizontal width of the beam. All beams are assumed to be identical. We assume that the plates and the beams are in constant contact, and thus we the conditions $w_1(x, y_j) = w_2(x, j) = w_3(x, y_j)$.

The energy contribution from the junctions is given by

$$\mathscr{P}_{1,2} = \frac{1}{2} \sum_{j=1}^{S} \int_0^A \sigma(x, j) \left| h_1 w_1'(x, y_j) + h_2 w_2'(x, j) \right|^2 dx \tag{5}$$

where σ is the Hooke's constants (though it is a function of x) for resistance for the slippage at the junction. The contribution from the beams and the bottom plate have the same formula except that the notation is $\mathscr{P}_{2,3}$ with the displacement functions w_2 and w_3. Finally the modified variational form from Eq. (1) is then given by

$$\delta^{(1)} \left[\mathscr{T} + \mathscr{P}_{1,2} + \mathscr{P}_{2,3} - \mathscr{V} - \mathscr{U} \right] = 0 \tag{6}$$

Now the terms $\mathscr{T}$ and $\mathscr{V}$ are the sum of all kinetic and strain energies of the plates and the beams.

The Fourier series solution

We now have to find the solution of Eq. (6) using the Fourier expansion method. The boundary of the plate is assumed to be simply supported. Thus the basis functions are sine-functions, which further simplifies the derivation of solutions. This section will show the derivation for the DLP because the single plate case is a simpler version of the DLP.

The displacement of the top plate and the beams can be expressed by

$$w_1(x, y) = \sum_{m,n,=1}^{N} C_{mn}^{(1)} \phi_m(x) \psi_n(y), \;\; w_2(x, j) = \sum_{m=1}^{N} C_{mj}^{(2)} \phi_m(x) \;\; j = 1, 2, \ldots, S, \tag{7}$$

, respectively. The basis functions are $\phi_m(x) = \sqrt{2/A} \sin k_m x$ and $\psi_n(y) = \sqrt{2/B} \sin \kappa_n y$. The series for the bottom plate w_3 is same as the series for w_1 except the sub- and super-scripts are changed from 1 to 3. The wavenumbers are given by $k_m = \pi m/A$ and $\kappa_n = \pi n/B$. Note that the basis functions are orthonormal. The positions of the joists are given by $y = y_j$, $j = 1, 2, \ldots, S$. We can derive the equations for the coefficients by substituting the series expansions into Eqs. (2), (4), (5) and then into Eq. (6). Note that the number of terms in the series has already been truncated to N to construct the finite system for the numerical computation.

The integrals can be expressed using the column vectors of the coefficients, which are, $\mathbf{c_1} = \left(C_{11}^{(1)}, \cdots, C_{NN}^{(1)}\right)^{\mathrm{t}}$, $\mathbf{c_2} = \left(C_{11}^{(2)}, \cdots, C_{NS}^{(2)}\right)^{\mathrm{t}}$, $\mathbf{c_3} = \left(C_{11}^{(3)}, \cdots, C_{NN}^{(3)}\right)^{\mathrm{t}}$ or simply denoted by the column vector $\mathbf{c} = (\mathbf{c}_1, \mathbf{c}_2, \mathbf{c}_3)$. The variational formulation then becomes

$$\delta^{(1)} \left\{ \frac{1}{2} \mathbf{c}^{\mathrm{t}} \mathbf{L} \mathbf{c} - \mathbf{p}^{\mathrm{t}} \mathbf{c} \right\} = 0 \tag{8}$$

where $\mathbf{L}$ is the matrix from the integrals and $\mathbf{p}$ is the vector of the external forcing and the super-script t indicates the vector transpose. The elements of $\mathbf{p}$ are given by the integral in Eq. (3),

$$\int_0^A \int_0^B p(x,y) \phi_m(x) \psi_n(y) \, dx dy, \;\; m,n = 1,2,...,N \tag{9}$$

with zero padding for the parts corresponding to $\mathbf{c}_2$ and $\mathbf{c}_3$ and thus the bottom $N^2 + N \times S$ elements are zero. In the numerical computations, the forcing will be set to be a point forcing, that is, $p(x,y) = \delta(x - x_0, y - y_0)$ for some fixed point (x_0, y_0), and thus the integrals are unnecessary. The coefficients are then found by solving the normal equation of Eq. (8),

$$\mathbf{L} \mathbf{c} = \mathbf{p} \tag{10}$$

Substituting the Fourier series expansion for the displacements w_1 and w_2 into Eq. (5) gives

$$\begin{aligned} \mathscr{P}_{1,2} = \frac{1}{2} \sum_{j=1}^{S} \sum_{\substack{m,n, \\ m',n'=1}}^{N} h_1^2 C_{mn}^{(1)} C_{m'n'}^{(1)*} \psi_n(y_j) \psi_{n'}(y_j) J_{mm'} + \frac{1}{2} \sum_{j=1}^{S} \sum_{m,m'=1}^{N} h_2^2 C_{mj}^{(2)} C_{m'j}^{(2)*} J_{mm'} \\ + \mathrm{Re} \sum_{j=1}^{S} \sum_{m,m',n=1}^{N} h_1 h_2 C_{mn}^{(1)} C_{m'j}^{(2)*} \psi_n(y_j) J_{mm'} \end{aligned} \tag{11}$$

where $J_{mm'} = k_m k_{m'} \int_0^A \sigma(x,j) \varphi_m(x) \varphi_{m'}(x) \, dx$ and $\varphi_m(x) = \sqrt{2/A} \cos k_m x$ and $*$ indicates the complex conjugate. The above integrals and summations can be rewritten using the vectors $\mathbf{c}_1$ and $\mathbf{c}_2$ and a matrix denoted by $\mathbf{L}_\sigma$,

$$\mathscr{P}_{1,2} = \frac{1}{2} \begin{pmatrix} \mathbf{c}_1 \\ \mathbf{c}_1 \end{pmatrix}^{\mathrm{t}} \mathbf{L}_\sigma \begin{pmatrix} \mathbf{c}_1 \\ \mathbf{c}_1 \end{pmatrix} \tag{12}$$

The matrix $\mathbf{L}_\sigma$ can be included as a part of the matrix $\mathbf{L}$ in Eq. (8).

NUMERICAL COMPUTATION OF SOLUTIONS

Simulation of irregularities based on power spectral density

We start with the simple discrete case when the plate is divided into grids as shown in Fig. 1 with a constant rigidity $\{D_{pq}\}_{p=1,...,P,q=1,...,Q}$, assigned for each grid. These sets of random numbers are assumed to be independent and have an identical PDF. The smooth functions for the rigidity and the slippage are also tested. In other words, the rigidity $D(x,y)$ in Eq. (2) can be rewritten to have a constant part and a zeros-mean random part. We then have $D(x,y) = \overline{D} + d(x,y)$, where $\overline{D}$ is the average rigidity and $d(x,y)$ is the random deviation. The slippage resistance function can also be expressed with the average and random deviation parts, $\sigma(x,j) = \overline{\sigma} + S(x)$. Note that the index j is omitted because the resistance for all beams will be randomized in the same way. These functions must be simulated with some PDF and PSD. We start with an 1-dimensional random function (process) $S(x)$. A parameter function with any PDF can be simulated using the method given in (Kay, 2010). However here only the Gaussian density function will used.

We assume that $S(x)$ has the probability $p(S \le s)$ and the PDF $p_S(s)$ at any $x \in [0, A]$. The PDF $p_S(s)$ is assumed to be identical for any x. In other words $S(x)$ is a stationary process. It is further assumed that $S(x)$ can be expressed by

$$S(x) = \sqrt{\frac{2}{M}} \sum_{i=1}^{M} Q_i \cos(2\pi F_i x/A + \Phi_i) \tag{13}$$

where Q_i, F_i, and Φ_i are the random variables with some probability densities. Here M needs to be sufficiently large, and is set to 100. The above series makes the mean of $S(x)$ zero for all $x \in [0, A]$.

The amplitudes $\{Q_i\}$ are assumed to be independent and identically distributed (i.i.d) random variable with PDF denoted by $p_Q(q)$ for $q > 0$. The phases $\{\Phi_i\}$ are also assumed to be i.i.d and their PDF is given by the uniform distribution in $[-\pi, \pi]$. The frequencies $\{F_i\}$ are i.i.d with the marginal first order continuous PDF denoted by $p_F(f)$ for $0 \le f \le V/2$. The PDF of F_i and the PSD of $S(x)$ denoted by $P_S(f)$ are related by the formula

$$p_F(|f|) = \frac{2}{\mathbb{E}\left[Q^2\right]} P_S(f), \ -V/2 \le f \le V/2 \tag{14}$$

where V is some large enough value so that $P_S(f)$ is nearly zero outside of the range $[-V/2, V/2]$. Setting the variance of S to be v^2 gives $\mathbb{E}\left[Q^2\right] = v^2$. The PSD function $P_S(f)$ here is chosen to be simple bell shaped. An example is shown in Fig. 3(left). The PDF of Q_i is given by $p_Q(q) = 2q/v^2 \exp\left(-q^2/v^2\right)$. This is a Rayleigh PDF, which can be simulated from the two Gaussian random variables. For example, when the variance is $v^2 = 2$, then the amplitudes are simulated by $U_1 \sim \mathcal{N}(0,1)$ and $U_2 \sim \mathcal{N}(0,1)$, then $Q \sim \sqrt{U_1^2 + U_2^2}$. The standard deviation of the distribution will be set to be 10% of $\overline{\sigma}$.

The random rigidity function $d(x, y)$ can be similarly simulated using the expansion

$$d(x,y) = \frac{2}{M} \sum_{i,j=1}^{M} Q_{ij} \cos(2\pi F_i x/A + \Phi_i) \cos\left(2\pi G_j y/B + \Psi_j\right) \tag{15}$$

where the coefficients $\{Q_{ij}\}$ are random variables with the Rayleigh distribution. In the numerical simulations, the standard deviation of the rigidity of the plates $d_1(x, y)$ and $d_3(x, y)$ will be set to be 10% of the average stiffness of the plates in the following section.

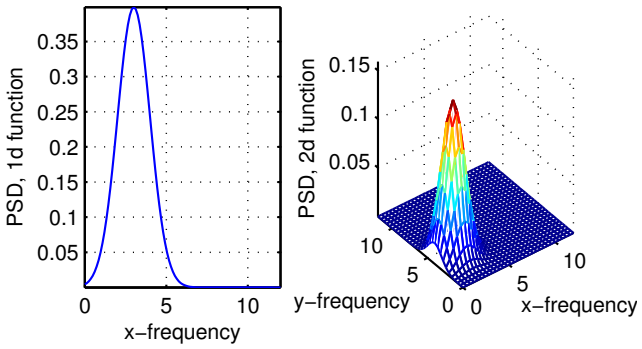

FIGURE 3: Examples of PSDs for the 1 and 2 dimensional random functions

Eigenvalue analysis

The number of terms for the Fourier expansion was set to be $N = 20$. All computation results are produced using MatLab on a standard desktop PC. The parameters for the beams and the

plates are chosen from the well used values for plywood and timber beams, $E_1 = E_3 = 10^{10}$ Pa, $E_2 = 1.4 \times 10^{10}$ Pa, $m_1 = m_2 = m_3 = 500$ kgm^{-3}, $A = 1.5$ m, $B = 2.5$ m, $h_1 = h_3 = 0.015$ m, $h_2 = 0.1$ m, $\nu = 0.3$, $y_j = jB/6$, $j = 1,2,...,5$, and the width of the beams is 0.05m. The average slippage constant is 3×10^7 Nm^{-1}, which was determined from the experiments in (Chung and Emms, 2008). The location of the forcing is $(1.07, 1.67)$ with $f_0 = 1000$ N. The range of the frequency is from 1 Hz to 1000 Hz with 0.5 Hz intervals.

For the single-plate cases, analysing the eigenvalues of the stiffness matrix lets us compare the effects of the random rigidity. The three cases of random rigidities are considered here. First, $D_{pq} \sim U(-1,1)$, i.e., D_{pq} has the uniform PDF in $[-1,1]$. Second, $D_{pq} \sim \mathcal{N}(0,1)$, i.e., D_{pq} has the Gaussian PDF with zeros mean and the standard deviation of 1. For these two cases $\{D_{pq}\}$ are assumed to be uncorrelated. Third, $d(x,y)$ at any (x,y) has the independent identical Gaussian probability density function, and the function d has the bell-shaped power spectral density function over $(x,y) \in [0,A] \times [0,B]$.

Figure 4 shows the mean fundamental frequencies α_n, $n = 1,2,...,100$ and their variance computed from the eigenvalues of the stiffness matrix. The mean of α_n is computed for the discrete and smooth rigidities. The PDFs of the discrete rigidity made little difference, whereas the smooth rigidity diverges as the frequency increases. The The amount of variance of the fundamental frequencies increases linearly for both uniformly and normally distributed rigidity as n increases. The smooth rigidity gives larger variance compared to the discrete cases when the standard deviation is the same 10% of the average rigidity.

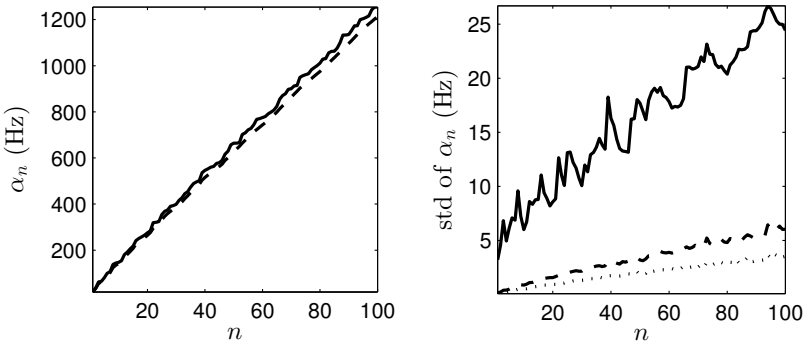

FIGURE 4: Left: the mean of the fundamental frequencies for the discrete (solid) and the smooth (dashed) random rigidities. Right: the standard deviation of the fundamental frequencies for uniformly distributed (dotted), normally distributed (dashed) and the smooth (solid) rigidities. The standard deviation of all three cases is 10% of $\overline{D}$.

Figure 5 shows the PDFs of α_{50} for the uniform, normal and smooth rigidities. The other $\{\alpha_n\}$ had the similar distribution. The fundamental frequency due to the discrete rigidities is normally distributed. Whereas α_{50} due to the smooth random rigidity has a skewed distribution. A set of examples are shown in Fig. 5. The skewness (always negative) increases as n increases.

Transmission-loss analysis

We here study the behaviour of the DLP using the transmission-loss (TL) between the top plate and the bottom one. The root-mean-square velocity (RMSV) of the plates are computed from the displacement w_1 and w_3, and then the TL of the DLP for various cases of random parameters are compared. The TL in this case is a simple log-ratio between the RMSV of the top and the bottom plates. The linearity of the system gives us the velocity of the plate by $v_1(x,y) = \mathrm{i}\omega w_1(x,y)$ (or $\mathrm{i}2\pi\alpha w_1(x,y)$) and same for v_3. Hence the RMSV can be computed by

$$\sqrt{\langle |v|^2 \rangle} = \frac{1}{\sqrt{AB}} \left[\int_0^B \int_0^A \omega^2 |w(x,y)|^2 \, dxdy \right]^{1/2} \tag{16}$$

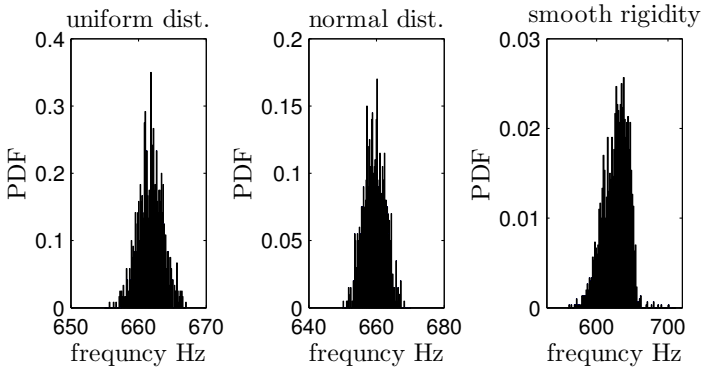

FIGURE 5: The PDF of 50th fundamental frequency for the uniform distribution (right), normal distribution (center) and smooth rigidity (right).

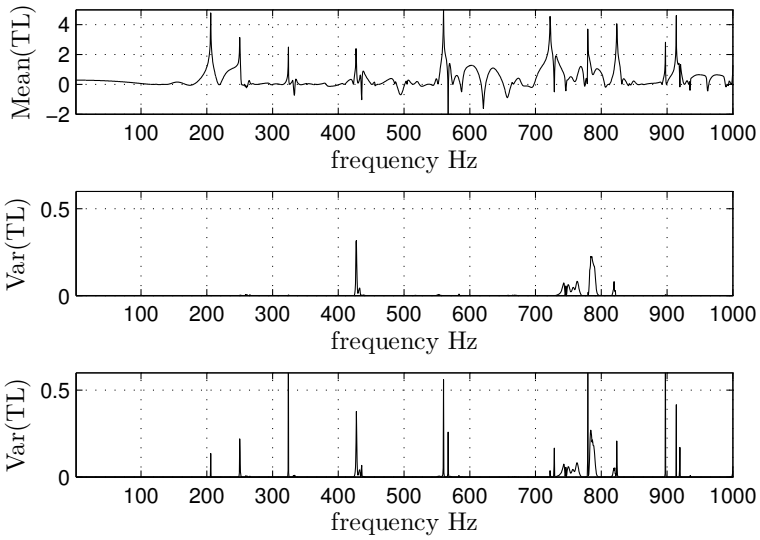

FIGURE 6: The mean of the TL (top). The variance of the TL when the slippage alone was randomized (middle) and both the slippage and the rigidities are randomized (bottom).

The above integral can be obtained using the simple Riemann sum once the displacement $w_1(x,y)$ and $w_3(x,y)$ have been computed. The TL is a function of frequency α, which is computed by

$$TL(\alpha) = \log_{10}\left[\sqrt{\langle|v_1|^2\rangle}/\sqrt{\langle|v_3|^2\rangle}\right] \tag{17}$$

Here we consider two cases when the slippage alone is randomized and both the slippage and the rigidity (both the top and the bottom plates) are randomized. The standard deviation of the slippage $S(x)$ is set to be 30% of the average slippage constant $\overline{\sigma}$. The random rigidities $d_1(x,y)$ and $d_3(x,y)$ are the same as before, which are set at 10% of the average rigidity. The TL and the variance of the TL are shown in Fig. 6. The mean of the TL changed little regardless of the randomization, and thus the smoothness of the rigidity made no difference to the mean TL. The variance of the surface velocity itself was much smaller than the single-plate cases shown in the previous section. The variance of the TL increases as the random rigidity is introduced the the DLP, though the variance has appreciable values mostly at the maxima of TL. The random rigidity affects the TL over a wider frequency range than the random slippage does.

Summary

The simulations of the vibration of elastic plates with random parameters have been carried out using the variational principle and the Fourier series expansion method. A single plate and a DLP have been considered. For the single plate, discrete and smooth rigidities are used to simulate their effects on the fundamental frequencies. The smooth rigidity gives larger variations in the fundamental frequencies than the discrete ones. Furthermore the distribution of the fundamental frequencies is skewed when the smooth rigidity is used. On the other hand, the discrete rigidities give normally distributed fundamental frequencies. The model for the DLP includes the slippage at the junctions between the beams and the plates as an additional energy. The computation method basically stays the same as the single-plate case because of the variational principle. The random slippage and the random rigidity are simulated from a pre-assigned PDF at each location and a PSD over either the beam or the plate. The TL is then used to study the effects of the randomness. The computational cost of computing the whole displacement and the average velocity is kept small using the Fourier series solutions and the variational formulation. The simulations show that the random rigidity affects the DLP less than it does the single plate. The mean of the TL remains the same regardless of the varying randomness in the slippage and the rigidity. The variance of the TL does show the difference in the effects between the slippage and the rigidity. The slippage affects narrower range of frequencies than the rigidity does.

References

Brunskog, J. (**2005**). "The influence of finite cavities on the sound insulation of double-plate structures", J. Acoust. Soc. Am **117**, 3727–3739.

Brunskog, J. and Chung, H. (**2011**). "Non-diffuseness of vibration fields in ribbed plates", J. Acoust. Soc. Am **129**, 1336–1343.

Chung, H. (**2012**). "Vibration field of a double-leaf plate with random parameter functions", Acoustics Australia **40**, 203–210.

Chung, H. and Emms, G. (**2008**). "Fourier series solutions to the vibration of rectangular lightweight floor/ceiling structures", Acta Acust. united Ac. **94**, 401–409.

Fahy, F. (**1994**). "Statistical energy analysis: A critical overview", Philos. Trans. R. Soc. London A: Physical and Engineering Sciences **346**, 431–447.

Kay, S. (**2010**). "Representation and generation of non-gaussian wide-sense stationary random process with arbitrary PSDs and a class of PDFs", IEEE Trans. Signal Processing, **58**, 3448–3458.

Lyon, R. (**1975**). *Statistical energy analysis of dynamical systems: theory and applications* (MIT Press, New York).

Mace, B. (**1980**). "Sound radiation from a plate reinforced by two sets of parallel stiffeners", J. Sound and Vibration **71**, 435–441.

Shames, I. and Dym, C. (**1991**). *Energy and finite element methods in structural mechanics*, si units ed. (Taylor & Francis, New York).

Wang, J., Lu, T., Woodhouse, J., Langley, R., and Evans, J. (**2005**). "Sound transmission through lightweight double-leaf partitions: theoretical modelling", J. Sound and Vibration **286**, 817–847.